Study of DSC, Ionic Conductivity, and ^{7}Li NMR Spectral Changes Associated with Cation Complexation in an Epoxide-Cross-Linked Polysiloxane/Polyether Electrolyte

Wuu-Jyh Liang and Ping-Lin Kuo*

Department of Chemical Engineering, National Cheng Kung University, Tainan, Taiwan 70101, ROC

Received August 24, 2003; Revised Manuscript Received November 29, 2003

ABSTRACT: Solid polymer electrolytes based on epoxide-cross-linked polysiloxane/polyether hybrid (SE55) were characterized by DSC, impedance measurements, and ^{7}Li MAS NMR spectra. The DSC results indicate that initially a cation complexation dominated by the cross-link site of SE55 is present, and subsequently the formation of transient cross-links between Li^+ ions and the ether oxygens of polyether segment results in an increase in T_g of the polyether segment (T_{g1}). However, the T_{g1} remains almost invariant at the highest salt concentration of O/Li^+ = 4. A VTF-like temperature dependence of ionic conductivity is observed in all of the investigated salt concentrations, implying that the diffusion of charge carrier is assisted by the segmental motions of the polymer chains, and furthermore, a maximum conductivity value is observed at O/Li^+ = 20 in the analyzed temperature range. Significantly, the ^{7}Li MAS NMR spectra provide high spectral resolution to demonstrate the presence of at least two distinct Li^+ local environments in SE55-based electrolytes. Detailed analyses of DSC and ^{7}Li MAS NMR spectra results are achieved and discussed in terms of ion−polymer and ion−ion interactions and further correlated with ion transport behavior.

Introduction

Solid polymer electrolytes (SPEs) can be obtained by the dissolution of salts in suitable ion-coordinating polymers.[1−3] Because of their great potential for applications in numerous electrochemical devices,[4] these materials have been intensively investigated during the past decade. Among the first and most studied host for SPE is poly(ethylene oxide) (PEO) due to its high solvating power and complexing ability to a wide variety of salts. Recognizing that the ionic conductivity of PEO-based electrolytes is facilitated in the amorphous phase of PEO, significant research effort has been devoted in tailoring a host structure having a highly flexible backbone and a larger proportion of the amorphous phase.[5−9] To prepare a SPE for practical applications, the high conductivity and the good physical properties such as chemical stability and mechanical strength have to be considered in the meantime regarding its structure.

Siloxane polymers having Si−O bonds are one of the candidates for materials of SPEs because they satisfy the requirements of having flexible main chains with a barrier to bond rotating being only 0.8 kJ mol^{-1}, very low glass transition temperature (e.g., −110 °C for a silicone rubber), and high chemical stability.[10] When polysiloxane segments are introduced into the main chain of the comblike polymers,[11] copolymers,[12] and cross-linked polymers,[13] the obtained polymer electrolytes have higher conductivity because of the flexibility of the polysiloxane segment. Recently, to acquire the high conductivity and the good physical properties of SPEs for practical applications, we have made an effort to produce ionic-conducting polymer electrolytes based on epoxide-cross-linked polysiloxane/polyether networks[14] with the aim to modulate the conductivity and physical properties of the materials by coupling suitable amounts of siloxane and PEO moieties along the polymer host. It indicated that the dependence of ionic conductivity on the composition is associated with the presence of structural heterogeneity of the hybrid networks. Although an understanding of the macroscopic properties associated with ion transport behavior in hybrid electrolytes has been investigated, in this study, we attempt to further elucidate the complex interplay between ionic transport process and interionic interactions. A detailed understanding of the role for ion−polymer/ion−ion interactions, the nature of the charge carrier, and the ionic association process in the ionic conductivity was examined by the DSC, impedance measurements, and ^{7}Li MAS NMR techniques.

* To whom all correspondence should be addressed: Tel +886-6-275 7575; Fax +886-6-276 2331; e-mail plkuo@mail.ncku.edu.tw.

Experimental Section

Materials. The epoxide−siloxane copolymer (SG80, EEW = 196 g/equiv) was prepared as described in our previous work.[15] Poly(ethylene glycol) diglycidyl ether (PEGDE, EEW = 290 g/equiv, Kyoeisha Chemical Co., Ltd.), polyoxypropylenediamine (Jeffamine D2000, AHEW = 514 g/equiv, Huntsman Corp.), and lithium perchlorate ($LiClO_4$, Aldrich) were dried at 80 °C under vacuum prior to use. All other chemicals were reagent grade and used as received, unless stated otherwise.

Sample Preparation. Mixtures of the epoxide precursors (SG80/PEGDE) with a weight ratio of 1:1 and the stoichiometric amount of PPO diamine (D2000) were dissolved in acetone and mechanically stirred for several minutes, and then the desired amount of lithium perchlorate ($LiClO_4$) was added. The mixed solution was cast onto aluminum plates, followed by evaporating the solvent at room temperature, and cured at 150 °C for 4 h. The thickness of the resulted films was controlled to be in the range 150−200 μm. These specimens were dried under vacuum at 80 °C for 72 h and then stored in an argon-filled glovebox (Vacuum Atmosphere Co.) for cell assembly. The undoped hybrid film (SE55) was also made in the same way without adding $LiClO_4$. Samples are labeled as SE55-*x*, where *x* refers to the molar ratio of ether oxygen to lithium perchlorate (O/Li^+). All of the resulted hybrid films

10.1021/ma035255m CCC: $27.50 © 2004 American Chemical Society
Published on Web 01/03/2004

Scheme 1. Schematic Structure of the Cross-Linked SE55 Hybrid (SG80:PEGDE = 1:1)

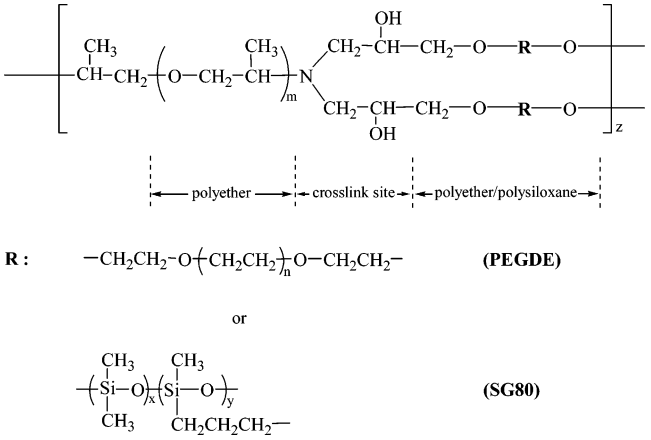

were flexible, transparent, and brownish. The schematic structure of polysiloxane/polyether hybrid is shown as Scheme 1.

Characterizations. DSC Studies. DSC data were recorded between −150 and +200 °C using a DuPont TA2010 differential scanning calorimeter with a low-temperature measuring head and a liquid nitrogen-cooled heating element. Samples in aluminum pans were stabilized by slow cooling to −150 °C and then heated at 10 °C/min to +200 °C. The glass transition zone was determined as the temperature range between two intersection points of the baselines with the extrapolated sloping portion of the thermogram, which resulted from a heat capacity change. Glass transition temperatures (T_g) were reported as the midpoint of the transition process. All the thermograms were baseline corrected and calibrated against indium metal. An empty aluminum pan was used as a reference.

Ionic Conductivity Measurements. Ionic conductivity was measured by an ac impedance technique using an electrochemical impedance analyzer (CH Instrument model 604A) under an oscillation potential of 10 mV from 100 kHz to 10 Hz. The samples were sandwiched between stainless steel blocking electrodes for conductivity tests. The impedance was measured in the temperature rang from 15 to 95 °C.

^{7}Li MAS NMR. ^{7}Li MAS NMR spectra were recorded with a Bruker AVANCE 400 spectrometer, equipped with a 7 mm double-resonance probe, operating at 400.13 MHz for ^{1}H and 155.5 MHz for ^{7}Li. Typical NMR experimental conditions were as follows: $\pi/2$ duration, 3 μs; recycle delay, 2 s; ^{1}H decoupling power, 65 kHz; spinning speed, 3 kHz. Chemical shifts were externally referenced to solid LiCl at 0.0 ppm.

Results and Discussion

DSC Studies. DSC was used to study the phase transitions of polymer electrolytes in order to correlate with the conductivity behavior and ^{7}Li MAS NMR spectra. Figure 1 shows the DSC curves obtained for the salt-free SE55 and SE55/$LiClO_4$ systems. The parent undoped SE55 shows two thermal transitions at very different temperatures. The lower temperature at ca. −60 °C (T_{g1}) is predominantly attributed to the motion of the polyether segments of the network, and the slight heat capacity change near 60 °C (T_{g2}) corresponds to the glass transition temperature of the network, above which mainly chain motion takes place, as usually observed for epoxy networks.[16−18] It is, however, difficult to distinguish between PEO and PPO segments since the difference in temperature is expected to be small. Moreover, the glass transition temperature of polysiloxane segments is not observed, possibly due to the relatively small content within the network. In the presence of $LiClO_4$, as evidenced in Figure 1, the

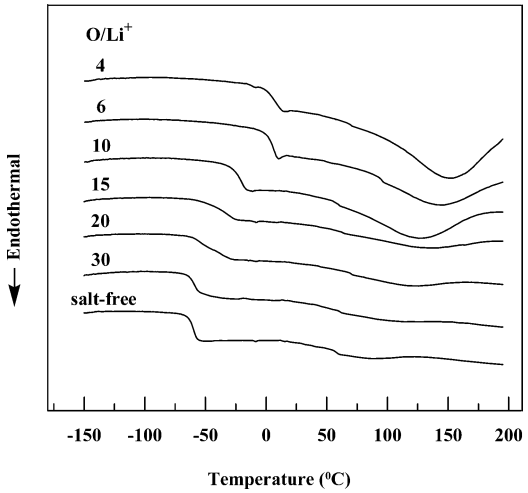

Figure 1. DSC curves for the salt-free SE55 and SE55/$LiClO_4$ complexes.

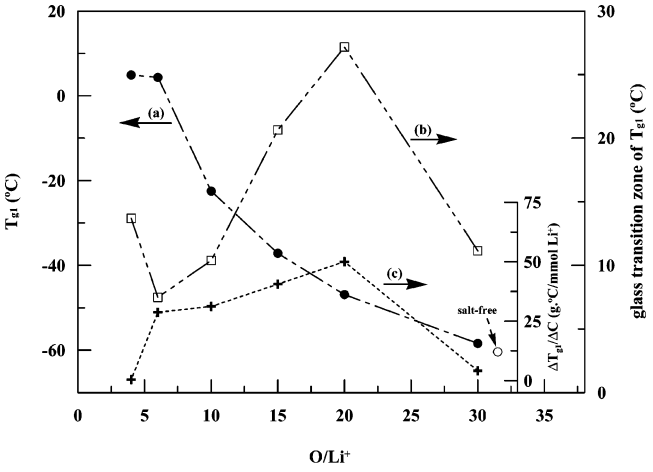

Figure 2. Variations in (a) T_{g1} (●), (b) glass transition zone of T_{g1} (□), and (c) $\Delta T_{g1}/\Delta C$ value (+) with salt concentrations for the undoped and $LiClO_4$-doped SE55.

thermal events change with increasing salt concentration. In comparison with the salt-free sample, a significant change in T_{g1} with increasing $LiClO_4$ concentration is observed. Nevertheless, this behavior is less accentuated for the T_{g2}. Also, at higher salt concentrations (O/Li^+ < 15), one high-temperature endotherm appears in the range 120−150 °C, ascribing to the melting temperature of the crystalline phase of the polyether−$LiClO_4$ complex.[19]

Figure 2 presents the variation in T_{g1} with salt concentration for the undoped and $LiClO_4$-doped SE55. As seen in Figure 2, the introduction of the salt in the polymer host leads to an increase in T_{g1} with increasing salt concentration up to O/Li^+ = 6, indicating a stiffening of the chain due to the ion−dipole interaction between the cation and the ether oxygens. At higher salt concentrations (O/Li^+ = 6 and 4), however, T_{g1} value almost remains invariant. This may be attributed to the plasticizing effect due to the formation of ion pairs or aggregations with increasing salt concentration.[20] Ion pairs or aggregates lose the ability to provide ionic crosslinks, and hence an obvious increase in T_{g1} is not observed further. In addition, the less pronounced increase in T_{g1} value is noticed when the salt concentration is increased from salt-free to O/Li^+ = 30, implying that the salt may interact preferentially with the crosslink site of polymer host at lower salt concentration.

This can be further confirmed by ^{7}Li NMR measurements shown below. With further addition of salt, the cation complexation in the polyether segment becomes more prominent, causing the raise of the rate of T_{g1} increase. Besides, the cations are expected to coordinate preferentially with the oxygens of PEO block because the solvating power of PEO is larger than that of PPO.

Figure 2 also displays the value of glass transition zone of T_{g1} varied with the $LiClO_4$ uptake. This value, obviously, reaches a maximum at salt concentration of $O/Li^+ = 20$ and thereafter shows a decreasing trend. However, this value dramatically increases at the highest salt concentration of $O/Li^+ = 4$. The glass transition zone is defined as the difference between the onset and endset temperatures of thermal transition process and reflects the number of relaxation processes associated with the transition. Complexed polyether units may be located randomly along the polyether segments. The mutual influences on the behaviors of the free and complexed polyether units probably undergo relaxation processes with different relaxation times, resulting in the broadening of the glass transition. At a relatively high $LiClO_4$ concentration, almost all polyether units are complexed with $LiClO_4$, and thus the distribution of the relaxation times becomes narrow again. In the concentrated salt concentration, the strong ion−ion interactions must exist. Consequently, the less mobile ion pairs and clusters are predicted to form, acting as transient cross-linking species. Such ion cluster transient cross-linkers probably not only interrupt the interaction between lithium cation and ether oxygen but also increase the distance between the polymer chains. These effects can be used to explain why the glass transition zone of T_{g1} increases at $O/Li^+ = 4$. Additionally, the $\Delta T_{g1}/\Delta C$ values, which are obtained by normalizing the T_{g1} data with respect to the concentration of $LiClO_4$ (in mmoles of $LiClO_4$ per gram of SE55), are also shown in Figure 2. Similarly, as seen in Figure 2, there exists a maximum for $O/Li^+ = 20$ and thereafter starts decreasing. At lower salt concentrations, Li^+ ions interact to a greater extent with polyether segment, casing an enhanced $\Delta T_{g1}/\Delta C$ change. Beyond the concentration ($O/Li^+ = 20$), the formation of ion pairs or aggregates results in a decrease in $\Delta T_{g1}/\Delta C$. Interestingly, ^{7}Li NMR spectroscopic analysis and ionic conductivity measurements (see below) also reveal the formation of contact ion pairs beyond the salt concentration of $O/Li^+ = 20$.

Ionic Conductivity Measurements. As usually observed for ionic conductors, electrical impedance plotted in the complex plane exhibits an arc of circle at higher frequencies that corresponds to the bulk conductivity of the samples, followed by an inclined linear variation at lower frequencies due to the interface between the sample and the blocking electrodes.[21] The intercept of the arc of circle with the real axis gives the ohmic resistance, from which conductivity can be deduced.

Figure 3 shows the variation of ionic conductivity with temperature for the SE55/$LiClO_4$ complexes. As is evident in Figure 3, the Arrhenius plots for ionic conductivity show VTF behavior ($\sigma = AT^{-0.5}\exp[-B/(T - T_0)]$),[22,23] which is indicative of ionic conductivity being coupled to polymer segmental motion.[24−28] Also, the conductivity of SE55-20 sample is the highest among the investigated samples throughout the temperature

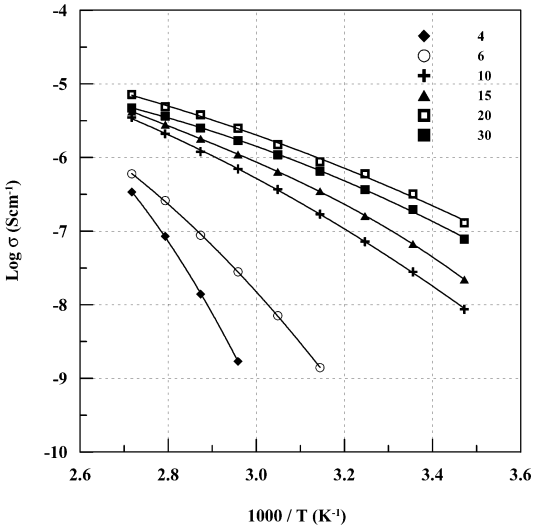

Figure 3. Variation of ionic conductivity with temperature for the SE55/$LiClO_4$ complexes.

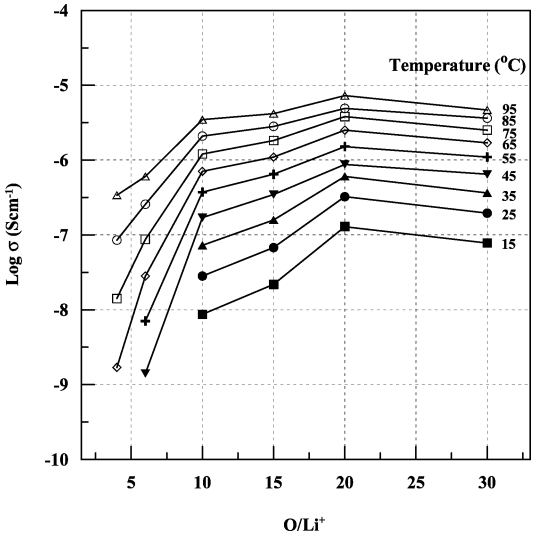

Figure 4. Salt concentration dependence of ionic conductivity under various temperatures from 15 to 95 °C for the SE55/$LiClO_4$ complexes.

range. The salt concentration dependence of conductivity is illustrated by examining isothermal plots as shown in Figure 4. Obviously, this system shows an increase in conductivity with salt concentration, and a maximum is observed at $O/Li^+ = 20$ in the analyzed temperature range 15−95 °C. Following the maximum, the conductivity decreases for higher salt concentrations. This feature is the reflection of two opposite effects, namely the increase in the number of charge carriers and the decrease in the free volume of polymer host.[29,30] As the concentration of salt is increased, the number of charge carriers is also increased, although the increase in charge carriers may not be a linear function of salt concentration if ion pairs or multiples formation is significant. Nevertheless, the average free volume is decreased as indicated from the increase in T_g owing to the interaction of Li^+ with ether oxygens. At low salt concentration level, the increase in the number of charge carriers dominates, and the decrease in free volume is compensated by the larger increase in the number of charge carriers. Hence, the conductivity is found to increase with salt concentration up to $O/Li^+ = 20$. With further increase in the salt concentration, the decrease

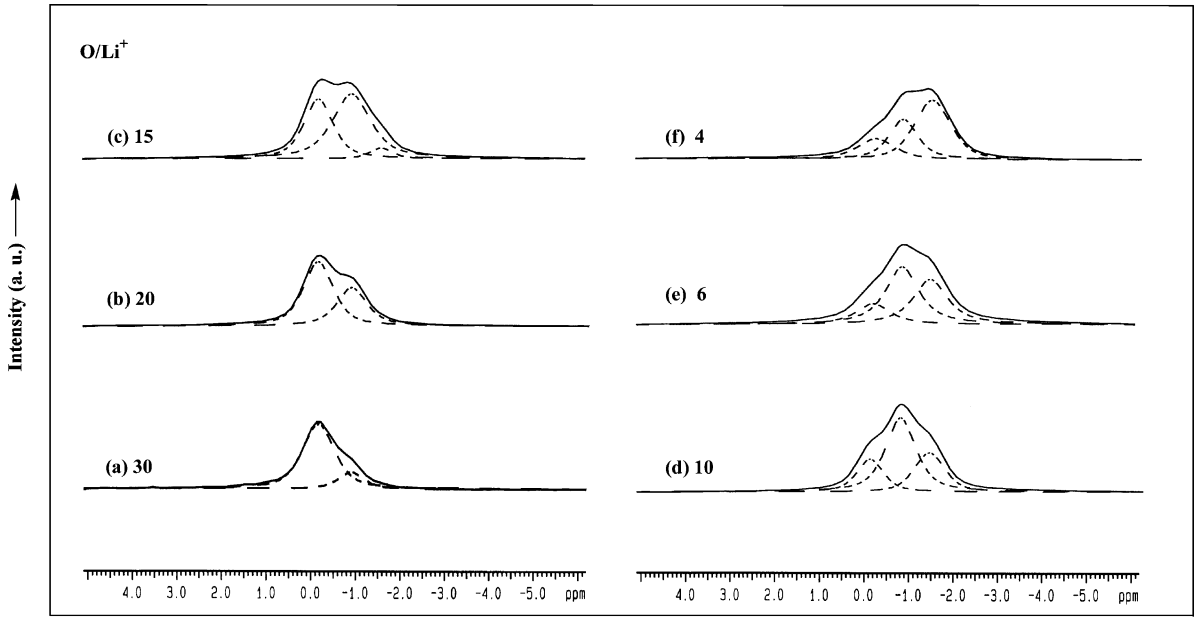

Figure 5. ^{7}Li proton-decoupled MAS NMR spectra of SE55/$LiClO_4$ complexes with various salt concentrations, recorded at 203 K.

in free volume becomes more pronounced than the increase in number of charge carriers. At this time, the lower fraction of free volume is no longer compensated by the continuous increase in the number of charge carriers. As a result, conductivity is decreased with the increase in salt concentration at higher salt concentration level. Additionally, at higher salt concentration considerable formation of ion pairs or aggregates decreases the number density of charge carriers present and also lowers the mobility of charge carriers throughout the polymer host; both effects result in a reduction in bulk ionic conductivity.

^{7}Li MAS NMR Spectra. ^{7}Li MAS NMR was used to acquire evidence for lithium cation complexation in the SE55/$LiClO_4$ system. The spectrum of a spin $^3/_2$ (e.g., ^{7}Li) system in a powdered crystalline sample is expected to consist of a narrow component due to the $^1/_2 \leftrightarrow -^1/_2$ transition and a Pake doublet due to the $^3/_2 \leftrightarrow {}^1/_2$ and $-^1/_2 \leftrightarrow -^3/_2$ satellite transitions.[31] Since the SE55 polymer is a heterogeneous system, the absence of the satellite quadrupole powder pattern could be due to a wide distribution of possible electronic field gradients which results in an almost unobservable Gaussian-broadened line shape for the satellite transitions at temperatures below the glass temperature. For this reason, only the ^{7}Li central transition was analyzed in this study. In addition, previous results[19] have indicated that the line width decreases significantly as the proton decoupling is applied on acquiring the ^{7}Li MAS NMR spectra due to a significant ^{7}Li$-^1$H dipolar interaction of lithium cations and polymer host. The central line broadening due to the second-order quadrupole interactions is expected to be small since its estimated contribution, ν_Q^2/ν_L, is on the order of hertz.[31] In this study, the proton-decoupled ^{7}Li MAS NMR spectra of SE55/$LiClO_4$ complexes as a function of salt concentration, recorded at 203 K, are displayed in Figure 5, together with the decomposed spectra by a mixture of Lorentzian/Gaussian fit to reveal the composition of lithium species. As seen in Figure 5a for the SE55 doped with the salt concentration of O/Li^+ = 30, the line shape is asymmetric, and two well-resolved components at −0.15 ppm (site I) and −0.90 ppm (site II) with integrated intensities of approximately 0.82:0.18 are observed, indicating that at least two distinct lithium species with different local environments exist in the polymer host, and the Li^+ cation is preferentially coordinated to site I. With further addition of $LiClO_4$ salt, as shown in Figure 5b−f, the line shapes significantly change with the variation of peak intensity with $LiClO_4$ uptake, and a shoulder (site III) lying at ca. −1.40 ppm becomes visible at higher salt concentrations.

Figure 6a shows the variation of the relative intensities of the three components with different salt concentrations, as determined from the deconvolution of NMR spectra with the accuracy estimated of ±5%. As seen in this figure, the relative intensity of site I decreases with increasing salt concentration, and furthermore, that of site II initially increases up to the concentration of O/Li^+ = 20 and then decreases in the higher salt concentration range. A decrease in relative intensity of site II accompanies an increase in relative intensity of site III. Since site III is only observed at higher salt concentrations and shows a concentration dependence of its intensity, site III is assigned to the ion pairs or aggregates. It is pertinent to note that the observed trend of the relative intensity in site II with increasing salt concentration is identical with the previous findings in ionic conductivity measurements. Figure 6b presents the amount of Li^+ cations with different local environments (in mmole per gram of SE55) under various $LiClO_4$ uptakes. It is noticed that the amount of Li^+ cations in site I is fairly constant at 0.4 mmol of $LiClO_4$ per gram of SE55, approaching to the quantity of cross-link site in SE55. Furthermore, the amount of Li^+ cations in site II increases with increasing salt concentration. Moreover, the amount of Li^+ cations in site III evidently increases with increasing salt concentration beyond O/Li^+ = 20. On the basis of the above-mentioned observations, it is reasonable to assume that as site I is saturated, then the excess Li^+ ions are coordinated to site II. More and more Li^+ ions are residing in site III as ion pairs or aggregates at higher salt concentrations. As shown in Scheme 1, except for ether oxygens in the polyether segments, the Li^+ ions could be coordinated to those nitrogen atoms or polar hydroxyl

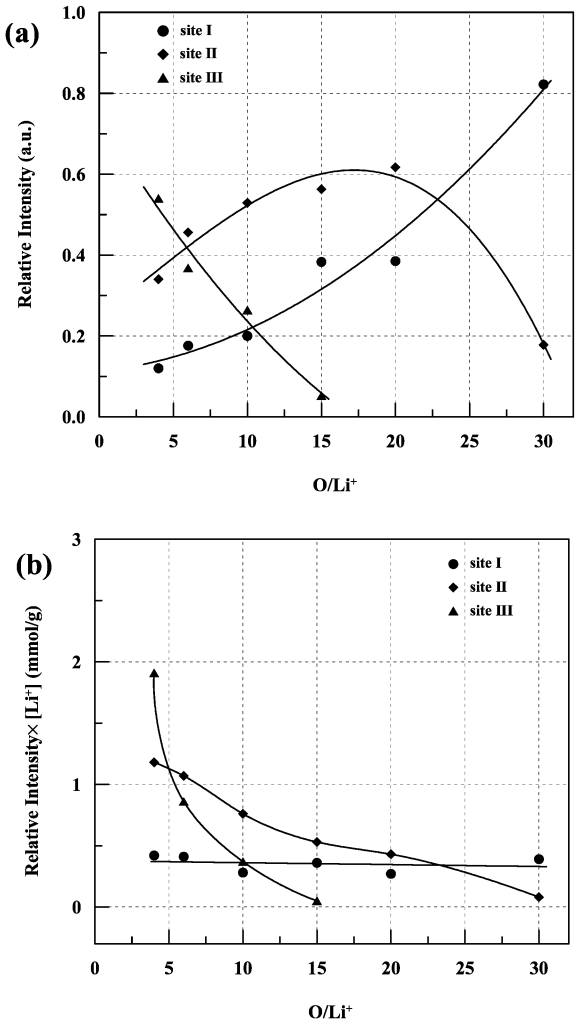

Figure 6. (a) Variation of the relative intensities of the three components with different salt concentrations, as determined from the deconvolution of NMR spectra with the accuracy estimated of ±5%. (b) Amount of Li^+ cations with different local environments under various $LiClO_4$ uptakes.

groups in SE55. The possibility of coordination with those silicon oxygens is excluded because of the reduced basicity by (p−d)π bonding from oxygen to silicon or hyperconjugation.[32] In fact, the nitrogen atom has a higher donicity (donor number ∼30) than ether oxygens (donor number ∼20),[33] and this should lead to a stronger complexing ability for the Li^+ cation; nevertheless, it tends to be not favorable for ion transport due to the steric hindrance effect of tertiary amine. Also, it was reported[34−36] that the Li^+ cations coordinated to −OH groups are more stable than those coordinated to ether oxygens in the polymer chains. On the basis of the fact that conductivity mainly resulting from the lithium cations in the polyether segment of SE55-based electrolytes, it can be concluded that site II is attributable to the Li^+ cations coordinated to ether oxygens in the polyether segments, while site I is associated with cross-link site in the polymer host. Furthermore, those observations in Figure 6 coincide with the previous DSC results which show a maximum for glass transition zone of T_{g1} and for $\Delta T_{g1}/\Delta C$ value at the salt concentration of $O/Li^+ = 20$ and that the coordination of cross-link sites might be preferentially formed at lower salt concentration, supporting the above assignments further.

Conclusions

The effect of changing salt concentration on the lithium cation complexation and ionic conductivity in solid polymer electrolytes based on epoxide-cross-linked polysiloxane/polyether hybrid has been investigated. These combined experiments point out that a strong correlation is observed between the behavior of the solid electrolyte and the Li^+ cation local environment. The obtained results are discussed in terms of ionic interactions, and a simple picture of ionic conduction is outlined. We propose the change in cation complexation regime from cross-link site environment at lower salt-doped level toward including polyether complexation, even the formation of ion clusters at higher salt concentration. This structural change promotes the decreases in ionic conductivity at higher salt concentrations.

Acknowledgment. The authors thank the National Science Council, Taipei, R. O. C., for their generous financial support of this research. The authors highly appreciated Ms. Ru-Rong Wu for her profound contribution in NMR experiments.

References and Notes

(1) Wright, P. V. *Br. Polym. J.* **1975**, *7*, 319.
(2) Armand, M. B.; Chabagno, J. M.; Duclot, M. J. In *Fast Ion Transport in Solids*; Vashista, P., Mundy, J. N., Shenoy, G. K., Eds.; Elsevier North-Holland: New York, 1979; p 131.
(3) Bruce, P. G.; Vincent, C. A. *J. Chem. Soc., Faraday Trans.* **1993**, *89*, 3187.
(4) Gray, F. M. *Polymer Electrolytes*; The Royal Society of Chemistry: London, UK, 1997; Chapter 5.
(5) Tada, Y.; Sato, M.; Takeno, N.; Nakacho, Y.; Shigehara, K. *Chem. Mater.* **1994**, *6*, 27.
(6) Inoue, K.; Nishikawa, Y.; Tanigaki, T. *Macromoelcules* **1991**, *24*, 3464.
(7) Blonsky, P. M.; Shriver, D. F.; Austin, P.; Allcock, H. R. *J. Am. Chem. Soc.* **1984**, *106*, 6854.
(8) Watanabe, M.; Rikukawa, M.; Sanui, K.; Ogata, N. *Macromolecules* **1986**, *19*, 188.
(9) Andrei, M.; Marchese, L.; Roggero, A.; Prosperi, P. *Solid State Ionics* **1994**, *72*, 140.
(10) Rochow, E. G. *Silicon and Silicones*; Springer-Verlag: Berlin, 1987.
(11) Fish, D.; Khan, I. M.; Wu, E.; Smid, J. *Br. Polym. J.* **1988**, *20*, 281.
(12) Nagaoka, K.; Naruse, H.; Shinohara, I.; Watanabe, M. *J. Polym. Sci., Polym. Lett. Ed.* **1984**, *22*, 659.
(13) Ogumi, Z.; Uchimoto, Y.; Takehara, Z. *Solid State Ionics* **1989**, *35*, 417.
(14) Liang, W. J.; Kuo, P. L., submitted for publication.
(15) Hou, S. S.; Chung, Y. P.; Chan, C. K.; Kuo, P. L. *Polymer* **2000**, *41*, 3263.
(16) Ochi, M.; Ozazaki, M.; Shimbo, M. *J. Polym. Sci., Polym. Phys. Ed.* **1982**, *20*, 689.
(17) Pogany, G. A. *Polymer* **1970**, *1*, 66.
(18) Enns, J. B.; Gillham, J. K. *J. Appl. Polym. Sci.* **1983**, *28*, 2567.
(19) Lin, C. L.; Kuo, P. L.; Wu, R. R.; Kao, H. M. *Macromolecules* **2002**, *35*, 3083.
(20) van Heumen, J. D.; Stevens, J. R. *Macromolecules* **1995,** *28*, 4268.
(21) Linford, R. G. *Electrochemical Science and Technology of Polymers*; Linford, R. G., Ed.; Elsevier Science: London, 1990; Vol. 2, p 281.
(22) Fulcher, G. S. *J. Am. Chem. Soc.* **1925**, *8*, 339.
(23) Watanabe, M.; Ogata, N. In *Polymer Electrolyte Reviews I*; MacCallum, J. R., Vincent, C. A., Eds.; Elsevier: London, 1987; Vol. 39, p 1987.
(24) Ratner, M. A. In *Polymer Electrolyte Reviews I*; MacCallum, J. R., Vincent, C. A., Eds.; Elsevier: London, 1987; p 173.

(25) Angell, C. A. *Solid State Ionics* **1983**, *9/10*, 3.
(26) Angell, C. A. *Solid State Ionics* **1995**, *18/19*, 72.
(27) Lonergan, M. C.; Shriver, D. F.; Ratner, M. A. *Electrochim. Acta* **1998**, *40*, 204.
(28) Mao, G.; Fernandez-Perea, R.; Howells, W. S.; Price, D. L.; Saboungi, M. L. *Nature (London)* **2000**, *405*, 163.
(29) Ferry, A.; Oradd, G.; Jacobson, P. *J. Chem. Phys.* **1998**, *108*, 7426.
(30) Cohen, M. H.; Turnbull, D. *J. Chem. Phys.* **1959**, *31*, 1164.
(31) Abragram, A. In *The Principles of Nuclear Magnetism*; Clarendon: Oxford, 1961.
(32) Bassindale, A. R.; Taylor, P. G. In *The Chemistry of Organic Silicon Compounds Part 1*; Patai, S., Rappoport, Z., Eds.; John Wiley & Sons: New York, 1989; Chapter 12.
(33) Gray, F. M. *Polymer Electrolytes*; The Royal Society of Chemistry: London, UK, 1997; p 12.
(34) Torell, L. M.; Jacobson, P.; Petersen, G. *Polym. Adv. Technol.* **1993**, *4*, 152.
(35) Manning, J.; Frech, R.; Huang, E. *Polymer* **1990**, *31*, 2245.
(36) Bernson, A.; Lindgren, J. *Polymer* **1994**, *35*, 4842.

MA035255M